Heliyon 10 (2024) e24705

Contents lists available at ScienceDirect

Heliyon

journal homepage: www.cell.com/heliyon

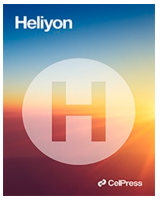

Research article

Prediction and optimization of hardened properties of concrete prepared with granite dust and scrapped copper wire using response surface methodology

Mohaiminul Haque, Sourav Ray [*,1], Ayesha Ferdous Mita, Anik Mozumder, Tirtha Karmaker, Sanjida Akter

Department of Civil and Environmental Engineering, Shahjalal University of Science and Technology, Sylhet, Bangladesh

ARTICLE INFO

Keywords:
Concrete
Granite dust
Scrapped copper wire
Strength
RSM
Optimization

ABSTRACT

Urban growth in the developing world has prompted researchers to seek alternatives to fine aggregate due to the severe environmental impact of extensive natural sand depletion. On top of that, the accumulation of non-biodegradable dumps, solid trash such as scrapped copper wire (SCW), and industrial remnants like granite dust (GD) have reached alarming levels. Therefore, incorporating these two waste materials in concrete offers a potentially sustainable solution. The study aims at substituting natural fine aggregate with GD as well as incorporating SCW for predicting and optimizing the compressive and splitting tensile strength of concrete using response surface methodology (RSM). Two independent variables, the volumetric percentages of GD (10 %, 20 %, and 30 %) and SCW (0.1 %, 0.3 %, and 0.5 %) in a concrete mix ratio of 1:1.5:3, were utilized to create probabilistic models for compressive and splitting tensile strength at 7 and 28 days. The experimental design employed central composite design (CCD) of RSM and the results of both ANOVA and regression analysis in terms of several statistical functions demonstrated a strong correlation between the predicted values of the responses and the actual experimental results. The developed models were validated by conducting experiments using optimized proportions of GD (23.32 %) and SCW (0.37 %). Finally, the strengths of the optimum content mix yielding 25.12 MPa and 3.266 MPa, respectively for compressive and splitting tensile at 28 days ensure the efficiency of the models due to the substantial similarity between experimental and predicted values. Therefore, integrating GD and SCW for higher-strength concrete in mass production can be a cost-effective alternative, fostering increased recycling of waste and supporting sustainable growth in building construction.

1. Introduction

In the preceding decades, rapid changes in modernization and population growth resulted in the enormous usage of concrete and its

* Corresponding author. Department of Civil and Environmental Engineering Shahjalal University of Science and Technology, Sylhet-3114, Bangladesh.

E-mail addresses: sourav.ceesust@gmail.com, sourav-cee@sust.edu (S. Ray).

[1] Postal Address: Sourav Ray Faculty Member Department of Civil and Environmental Engineering Room No: 108, Academic Building-'C' Shahjalal University of Science and Technology, Sylhet-3114, Bangladesh.

https://doi.org/10.1016/j.heliyon.2024.e24705
Received 30 July 2023; Received in revised form 12 December 2023; Accepted 12 January 2024
Available online 14 January 2024

widespread need for basic materials. Since 2005, almost six billion tons of annual concrete production have occurred, which equates to almost one ton per capita [1]. As the demand for aggregates dramatically increased, natural resources used as basic constituents of concrete are also being depleted remarkably [2]. Ordinary concrete generally comprises around 12 % cement and 65–70 % aggregate by mass [3]. Production of concrete globally consumes gravel, sand, and crushed rock of about 10–11 billion tons every year [4]. Most fine aggregates come from natural resources like river sand [4]. The widespread degradation of natural sand reserves causes environmental issues such as riverbank erosion and collapse, riverbed lowering, and saltwater intrusion into the soil [5]. Therefore, the inclusion and substitution of recycled waste materials in the construction industry can be an efficient approach topromoting an eco-friendly environment [6–11].

Granite dust, generated from granite industries, comes as a by-product throughout the preparatory process of cutting and polishing granite products [12] Around 78 million tons of granite and marble stone waste are generated annually worldwide [13]. However, unsafe, untreated disposal of granite waste results in harmful environmental impacts [14]. However, GD previously used in concrete substituting cement showed the highest increment in strength up to 10 % replacement [15] Furthermore, granite dust utilized as a partial substitution for fine aggregate results in significant improvement or modification in concrete's mechanical properties. Most studies demonstrate that concrete mixes with a 30 % substitution of natural fine aggregates with granite fines had the maximum compressive strength [16–20], which is attributed to a stronger physical connection between the binder and angular-shaped granite granules [21]. Another study conducted by Jain et al. exhibited improvement in mechanical performance in self-compacting concrete up to 40 % Granite waste [22]. Divakar et al. observed that, with a 35 % replacement of fine aggregates by granite dust, concrete's compressive strength increased by 22 %; however, with a 50 % substitution, the compressive strength increased by only 4 % [23]. Therefore, the compressive strength rises apparently with the percentage of granite dust in the concrete mix raised to 20 %. If the sand replacement level exceeds 25 %, the splitting tensile strength falls [24–27]. However, a study conducted by Ghannam et al. [17] shows that the highest compressive and splitting tensile strength values were achieved when granite dust replaced 10 % and 15 % of the sand, respectively. Again, the findings showed that fine aggregate's 9 % substitution by granite fines yields more compressive and splitting tensile strength than ordinary concrete [28].

Moreover, concrete is commonly known as a brittle material, and adding fibers to the concrete matrix restrains its brittleness, increases tensile performance and toughness, and improves ductility [29,30]. Therefore, fibers have been increasingly employed in concrete construction to address the inherent tensile strength and hardness abridgements in ordinary concrete in recent years [31]. In previous studies, fiber-reinforced concrete (FRC) has also shown favorable compression and tensile behavior [32–36].

Recycling fibers from industrial or post-consumer waste implies further waste reduction and resource conservation benefits [37]. A massive amount of electrical and electronics waste is produced every year globally, which will be around 52.2 million tons by the year 2021 [38]. Most of them are scrapped copper wire which can be an effective fiber-reinforcing material. Currently, steel fiber-reinforced concrete is more widely utilized and researched than other types of fibers [35,39–41]. But corrosion of steel fibers is a drawback that can affect the overall performance of concrete [42,43]. So, it will be more suitable if less corrosive materials can be used. Shende et al. [44] found that compressive strength, flexural strength, and splitting tensile strength are on the upper end of the scale for 3 % of steel fibers. Another study shows that for 65 and 80 aspect ratios, the compressive strength of concrete increases up to 1 % of steel fiber volume, and the splitting tensile strength of concrete rises to 1.5 % volume of steel fiber [45]. However, Sobuz et al. [46] incorporated copper wire in SCC made with rice husk ash and found the maximal strength at 1 %.

RSM is one such statistical analytic optimization technique that works effectively when one or more yield components are influenced by multiple independent factors [47]. RSM is an efficient method that allows mathematical and statistical approaches for establishing an appropriate functional relationship within a response and a set of governing variables, and its goal is to maximize or minimize this response [48–50]. Previously, Elemam et al. [51] optimized high-strength geopolymer concrete containing clay brick powder and fine clay brick by the RSM approach. Awolusi et al. [35] employed RSM to predict and optimize concrete made with limestone powder and steel fiber obtained from waste tires. Ahmed et al. [43] used RSM for the goal of predicting and optimizing concrete made with condensed milk can fiber and glass waste. Haque et al. [52] predicted and optimized the fresh and hardened characteristics of concrete consisting of rice husk ash and glass fiber by adopting RSM. Through the performance of the multi-response application, the percentage of standard ready-mixed concrete has been optimized by RSM [53]. Amiri et al. [54] employed RSM as a multi-objective optimization tool for the recycling of coal waste in concrete.

In light of the facts mentioned above, an initiative has been taken here to reuse GD and SCW as concrete constituents and investigate the impact of these two waste materials on the concrete hardened properties. Despite having different research on the individual impacts of introducing GD and SCW in concrete conducted previously, no studies regarding their combined effects have been done yet. Therefore, this paper aims to utilize these two poorly managed waste materials i.e. GD and SCW combinedly to produce high-strength concrete. The experimental data for all the responses i.e. compressive strength and splitting tensile strength were collected and employed to construct mathematical models. Subsequently, these models underwent statistical evaluation through ANOVA and were validated accordingly. The optimal proportions of GD and SCW in the concrete mix have also been determined bymaximizing the utilization of GD and SCW to enhance the desired concrete properties. Thus, this study not only outlines the methodology for producing concrete with greater strength potential but also assures environmental sustainability through waste recycling practices.

Fig. 1. Used materials: (i) 10 mm stone, (ii) 20 mm stone, (iii) Coarse sand, (iv) Medium sand, (v) Granite dust, (vi) Scrapped copper wire.

2. Materials and methods

2.1. Materials

As a binding material, 52.5 N ASTM C150 Type – 1 Ordinary Portland Cement (OPC) was employed in concrete. Stone chips were used as coarse aggregates having a size of 20 mm and 10 mm downgraded with a combination of 70 % and 30 %, respectively. River sand (Sari River) with particle sizes varying from 0.075 mm to 4.75 mm was employed as fine aggregate. The water used for the concrete mixing was at room temperature. GD, containing particles ranging in size from 0.075 mm–4.75 mm, was collected from a local granite refining industry (Green Granite and Marble Ltd.). Furthermore, SCW was collected from the local waste garage as a fiber added to the mix. Collected wires (0.70 mm diameter) were cut into 30 mm lengths to use in the concrete samples (see Fig. 1). The properties of the constituent materials are provided in Table 1.

2.2. Mix proportions

Table 2 represents the 13 concrete mix ratios used in the present study. The fine aggregates were partially replaced by GD in concrete at three different proportions of 10 %, 20 %, and 30 %. In addition, three distinct volumetric percentages of SCW (0.1 %, 0.3 %, and 0.5 %) were added as fiber reinforcement. Concrete mixes have been made with a constant water-cement ratio (W/C) of 0.50 and a design mix ratio of 1:1.5:3. In this research work, all the ingredients were mixed according to their volume fraction percentages.

2.3. Testing methods

Test specimens were produced in cylindrical casting molds having dimensions of 100 mm × 200 mm for all the strength assessments. Grease was applied to allow simple demolding and prevent concrete from adhering to the molds. The fresh concrete mix was deposited in two layers, and each layer received 25 blows from a tamping rod. After casting, the concrete samples were left to dry for 24 h. After being demolded, the specimens were submerged in fresh water for 7–28 days for the curing process. Fig. 2 visually represents the process. For each mix proportion, three specimens were prepared and a total of 156cylinder specimens were cast. Afterward, tests for compressive and splitting tensile strength were performed following ASTM C39 and ASTM C496, respectively.

2.4. Experimental design by RSM

In RSM, central composite designs (CCD) are used to efficiently generate a second-order model or a quadratic model. When a first-order model fails to fit owing to the lack of interaction between components and surface curvature, a quadratic or second-order model can considerably enhance the optimization process. To determine the correlation between factors and the response, the quadratic

Table 1
Properties of constituent materials of concrete.

Name of property	Unit	Sand	Stone	GD	SCW
Density (OD)	kg/m^3	2577	2763	2513	–
Density (SSD)	kg/m^3	2656	2788	2558	–
Bulk Density	kg/m^3	1596	1621	1620	8500
Water absorption Capacity	%	2.88	0.91	1.78	–
Specific Gravity (OD)	–	2.58	2.76	2.52	–
Specific Gravity (SSD)	–	2.66	2.79	2.56	–

Table 2
Concrete mix proportion.

Mix Name	Cement(kg/m^3)	Coarse Aggregate(kg/m^3)	Fine Aggregate (kg/m^3)			SCW (kg/m^3)		W/C Ratio	Water(kg/m^3)
			Sand	Granite Dust	% Replaced	Fiber	Volumetric % of Fiber		
G1	399.6	1198.8	539.46	59.94	10	2.40	0.1	0.5	199.8
G2	399.6	1198.8	479.52	119.88	20	2.40	0.1		199.8
G3	399.6	1198.8	419.58	179.82	30	2.40	0.1		199.8
G4	398.8	1196.4	538.38	59.82	10	7.18	0.3		199.4
G5	398.8	1196.4	478.56	119.64	20	7.18	0.3		199.4
G6	398.8	1196.4	478.56	119.64	20	7.18	0.3		199.4
G7	398.8	1196.4	478.56	119.64	20	7.18	0.3		199.4
G8	398.8	1196.4	478.56	119.64	20	7.18	0.3		199.4
G9	398.8	1196.4	478.56	119.64	20	7.18	0.3		199.4
G10	398.8	1196.4	418.74	179.46	30	7.18	0.3		199.4
G11	398.0	1194.0	537.31	59.70	10	11.94	0.5		199.0
G12	398.0	1194.0	477.61	119.40	20	11.94	0.5		199.0
G13	398.0	1194.0	417.91	179.10	30	11.94	0.5		199.0

Fig. 2. Preparation and curing of the concrete cylinder specimens.

model (Eq. (2.1)) was utilized in this study.

$$y = \beta_0 + \sum_{i=1}^{k} \beta_i x_i + \sum\sum_{i<j} \beta_{ij} x_i x_j + \sum_{i=1}^{k} \beta_{ii} x_i^2 + \epsilon \tag{2.1}$$

Here, β_0 is a constant, β_i stands for linear coefficient, β_{ii} represents quadratic coefficient and β_{ij} is an interactive coefficient.

Table 3
Governing factors and level of factors for RSM.

Factor	Code	Level of factors		
		Low	Intermediate	High
		−1	0	+1
GD content (%)	A	10	20	30
SCW content (%)	B	0.1	0.3	0.5

The response surface approach was utilized in this investigation to determine the impacts of GD and SCW on concrete strength using Design-Expert, Stat-Ease, Inc. software. GD content (%) and SCW content (%) were entered as numerical factors and the responses were coded as strength. Each response was determined using a face-centered CCD with an alpha (α) value of 1. Table 3 displays the components and the levels of independent variables.

Table 4 lists the experimental runs, their factor combinations, the space types employed in this investigation, and the conversion of coded levels into real experimental units.

2.5. Statistical parameters for evaluation of predicted data

Several statistical measures such as the coefficient of determination (R^2), mean square error (MSE), coefficient of correlation (R), root mean square error (RMSE), mean absolute error (MAE), average error (AE), and standard error prediction (SEP), were implemented to evaluate the functionality of the RSM model [55–57]. All these metric equations are elaborated in equations (2.2)-(2.8).

$$R = \frac{\sum_{1}^{n} (x\text{-}\overline{x})(x_i\text{-}\overline{x_i})}{\sqrt{\sum_{1}^{n} (x\text{-}\overline{x})^2 \sum_{1}^{n} (x_i\text{-}\overline{x_i})^2}} \tag{2.2}$$

$$R^2 = \left(\frac{\sum_{1}^{n} (x\text{-}\overline{x})(x_i\text{-}\overline{x_i})}{\sqrt{\sum_{1}^{n} (x\text{-}\overline{x})^2 \sum_{1}^{n} (x_i\text{-}\overline{x_i})^2}} \right)^2 \tag{2.3}$$

$$MSE = \frac{\sum_{1}^{n} (x_i - x)^2}{n} \tag{2.4}$$

$$RMSE = \sqrt{\frac{\sum_{1}^{n} (x_i - x)^2}{n}} \tag{2.5}$$

$$MAE = \frac{1}{n} \sum_{1}^{n} |x_i - x| \tag{2.6}$$

$$AE = \frac{1}{n} \sum_{1}^{n} (x_i\text{-}x) \tag{2.7}$$

$$SEP = \frac{RMSE}{\overline{x}} * 100 \tag{2.8}$$

Here, n refers to the number of observations or mix proportions. x and $\overline{x}$ represent the actual and average of actual data, x_i, $\overline{x}$ and $\overline{x_i}$ represent the predicted and average of predicted data, respectively. Fig. 3 demonstrates the sequential process diagram of this research.

Table 4
Factor composition in RSM according to the face-centered central composite design (CCD).

Run	Space type	Coded		Actual	
		GD (A)	SCW (B)	GD %	SCW %
1	Center	0	0	20	0.3
2	Factorial	−1	−1	10	0.1
3	Factorial	−1	1	10	0.5
4	Factorial	1	1	30	0.5
5	Center	0	0	20	0.3
6	Factorial	1	−1	30	0.1
7	Center	0	0	20	0.3
8	Axial	0	−1	20	0.1
9	Axial	1	0	30	0.3
10	Center	0	0	20	0.3
11	Axial	0	1	20	0.5
12	Axial	−1	0	10	0.3
13	Center	0	0	20	0.3

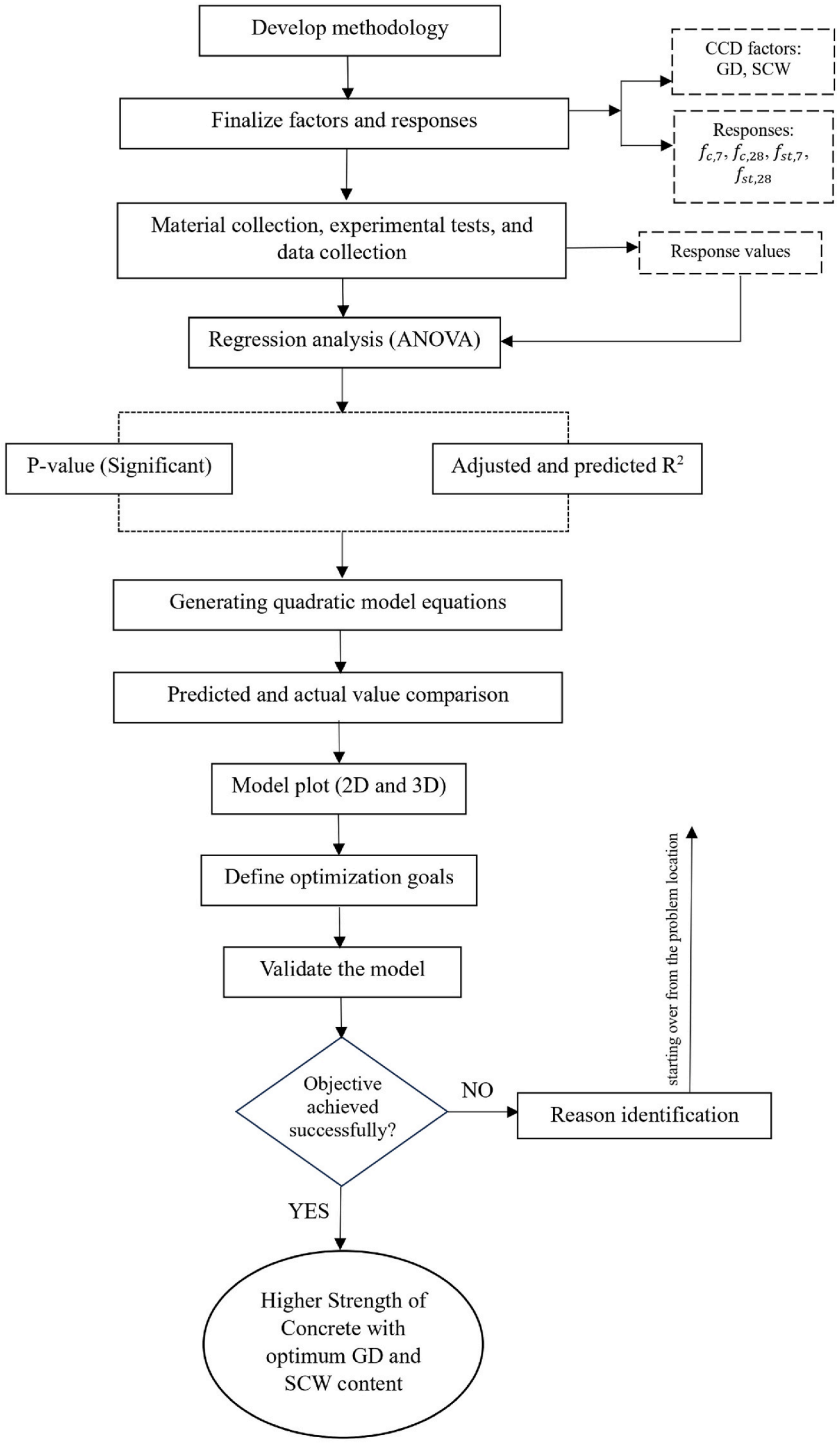

Fig. 3. Work process flow diagram.

3. Result and discussion

3.1. Assessment of RSM models

In this study, the impact of input variables on concrete strength as desired responses were determined by employing RSM. Tables 5 and 6 demonstrate the experimental run of the variables and the observed and predicted data of all the responses desired.

Table 5
Observed and predicted values of compressive strength, f'_c at 7 and 28 days.

Run order	GD %	SCW %	Compressive Strength (MPa)			
			7 days		28 days	
			Observed	Predicted	Observed	Predicted
1	20	0.3	16.04	16.11	24.47	24.51
2	10	0.1	13.15	13.01	21.06	20.88
3	10	0.5	13.72	13.67	21.74	21.46
4	30	0.5	16.20	16.25	24.31	24.45
5	20	0.3	16.15	16.11	24.53	24.51
6	30	0.1	15.67	15.64	23.12	23.16
7	20	0.3	16.10	16.11	24.54	24.51
8	20	0.1	14.70	14.97	22.51	22.66
9	30	0.3	16.90	16.77	25.37	25.18
10	20	0.3	16.15	16.11	24.41	24.51
11	20	0.5	15.50	15.61	23.66	23.60
12	10	0.3	13.90	14.16	22.28	22.55
13	20	0.3	16.10	16.11	24.69	24.51

Table 6
Observed and predicted values of split tensile strength, f_{st} at 7 and 28 days.

Run order	GD %	SCW %	Splitting Tensile Strength (MPa)			
			7 days		28 days	
			Observed	Predicted	Observed	Predicted
1	20	0.3	1.861	1.855	3.276	3.288
2	10	0.1	1.627	1.635	2.801	2.802
3	10	0.5	1.778	1.791	3.128	3.136
4	30	0.5	1.658	1.663	2.936	2.943
5	20	0.3	1.858	1.855	3.285	3.288
6	30	0.1	1.598	1.598	2.832	2.831
7	20	0.3	1.851	1.855	3.267	3.288
8	20	0.1	1.805	1.797	3.083	3.083
9	30	0.3	1.639	1.634	2.988	2.981
10	20	0.3	1.860	1.855	3.296	3.288
11	20	0.5	1.924	1.907	3.321	3.305
12	10	0.3	1.736	1.716	3.073	3.063
13	20	0.3	1.820	1.855	3.301	3.288

The polynomial equation of second-order represents the multiple regression analysis regarding the experimental findings of four responses based on CCD experimental design. Equations (3.1)–(3.4) express the equations for the compressive strength at 7 days ($f'_{c,7}$) and at 28 days ($f'_{c,28}$), And also splitting tensile strength at 7 days ($f_{st,7}$), and at 28 days ($f_{st,28}$), respectively.

$$f'_{c,7} = 16.108 + 1.303A + 0.317B - 0.645A^2 - 0.821B^2 \quad (3.1)$$

Table 7
ANOVA results for response surface model of compressive strength (MPa).

Source	7 days				28 days			
	SS	df	F-value	P-value	SS	df	F-value	P-value
Model	15.62	5	179.51	<0.0001	21.56	5	126.67	<0.0001
A-GD	10.19	1	585.39	<0.0001	10.43	1	306.31	<0.0001
B-SCW	0.6047	1	34.74	0.0006	1.32	1	38.77	0.0004
A^2	1.15	1	66.02	<0.0001	1.14	1	33.44	0.0007
B^2	1.86	1	107.05	<0.0001	5.27	1	154.91	<0.0001
Residual	0.1218	7			0.2383	7		
Lack of Fit	0.0992	3	5.83	0.0608	0.1956	3	6.11	0.0564
Pure Error	0.0227	4			0.0427	4		
Cor Total	15.74	12			21.80	12		
R^2	0.9923				R^2	0.9891		
Adjusted R^2	0.9867				Adjusted R^2	0.9813		
AP	41.919				AP	34.370		

SS = Sum of Square; AP = Adequate precision; df = degree of freedom.

$$f'_{c,28} = 24.508 + 1.318A + 0.469B - 0.642A^2 - 1.3172B^2 \quad (3.2)$$

$$f_{st,7} = 1.855 - 0.041A + 0.055B - 0.023AB - 0.180A^2 \quad (3.3)$$

$$f_{st,28} = 3.288 - 0.041A + 0.111B - 0.056AB - 0.266A^2 - 0.094B^2 \quad (3.4)$$

Here, A and B represent GD (%) and SWC (%), respectively.

Analysis of variance (ANOVA) with a 95 % confidence level was executed to determine the significance of the simulation model and its terms. Tables 7 and 8 represent the findings of ANOVA, where the P-values are substantially lower than 0.05 in all models, which means that all models are significant. On the contrary, the superior the F-value in an ANOVA, the more significant the difference between sample averages compared to the range within the samples, which means the lower the P-value [49]. The F-values of all models are significantly high (179.51, 126.67, 82.01, and 439.22), which means the null hypothesis of the ANOVA can be rejected and there is a statistically significant variation between group means [50]. The lack-of-fit value for all four responses is higher than 0.05, which indicates that the lack of fit for all cases is insignificant. Such non-significant lack of fit depicts good prediction capability in the model, so the developed models have strong prediction capability i.e., significant [51].

3.2. Analysis of responses using RSM

From the ANOVA results, it has been shown that the P-value is < 0.05 for the linear as well as quadratic impacts of A and B (A, B, A^2, and B^2). As a model term is significant for P-value <0.05, all these impacts are significant. Table 5 displays the observed and predicted values for f'_c observed at 7 and 28 days. The f'_c at 7 and 28 days rose from 13.01 to 16.77, and 20.88 to25.18 MPa along with the increase of GD content from 10 % to 30 % and the increase of SCW content from 0.1 % to 0.3 %, respectively. These values further decline to 16.20 and 20.31 MPa, respectively, with a further rise in SCW content (0.5 %). Figs. 4 and 5 depict the response surfaces and contour plots of compressive strength found at both 7 and 28 days after the curing.

Figs. 4 and 5 indicate the ideal correlation among the independent variables that are shown by the elliptical shaping of the contours of compressive strength. As per these 3D plots, f'_c has grown significantly along with expanding GD percentage up to the optimal content (30 %). The curve in the 3D graphs exhibits that the increasing rate of compressive strength is slowly decreasing. Several studies by Ghannam et al. [12], Singh et al. [17], and Vijaylakshmi et al. [58] show a similar pattern in compressive strength for concrete having GD as a substitue for fine aggregate. The compactness of the dense cement-aggregate matrix and the optimal C–S–H gel concentration contribute the most to emphasizing the best compressive strength of concrete mixed with GD [20]. An excessive quantity of cement was needed to bond the fine GD aggregate phase inside the concrete matrix due to its increased surface area. Since the cement content was maintained constant in every mix; the strength pattern was found to be decreasing at higher replacements of fine aggregate [52]. According to the 3D plot (Figs. 4 and 5), the compressive strength increases with the SCW increment until a specific point (0.3 %), and following this proportion increasing to 0.5 % of SCW, strength decreases along. Song and Hwang [53] reported a similar phenomenon with concrete containing steel fiber. This improved mechanical performance of concrete might result from the formation of cement hydration on fiber surfaces and the solid connection between fiber and cement matrix [43]. However, excessive fiber inclusion leads to pervious concrete, which weakens the bonding between constituents of concrete [54].

The contours of splitting tensile strength in Figs. 6 and 7 illustrate the relations between independent factors. Applying the P-value approach for splitting tensile strength, the terms A, A^2, B, and AB are significant statistically for responses of both 7 days and 28 days and the impact of quadratic term B^2 retains its significance when splitting tensile strength after 28 days is observed. Figs. 6 and 7 show that a simultaneous increase in GD content from 10 % to 30 % and SCW content from 0.1 % to 0.5 % increases the f_{st} at both 7 and 28 days. But if GD content is increased up to 30 %, values avowedly decrease to 1.66 and 2.94 MPa at 7 and 28 days, respectively. Again,

Table 8
ANOVA results for response surface model of splitting tensile strength (MPa).

Source	7 days				28 days			
	SS	df	F-value	P-value	SS	df	F-value	P-value
Model	0.1368	5	82.01	<0.0001	0.4157	5	439.22	<0.0001
A-GD	0.0101	1	30.22	0.0009	0.0102	1	53.63	0.0002
B-SCW	0.0183	1	54.94	0.0001	0.0744	1	392.80	<0.0001
AB	0.0021	1	6.21	0.0414	0.0124	1	65.30	<0.0001
A^2	0.0896	1	268.54	<0.0001	0.1953	1	1031.88	<0.0001
B^2					0.0245	1	129.51	<0.0001
Residual	0.0023	7			0.0013	7		
Lack of Fit	0.0012	3	1.35	0.3778	0.0005	3	0.9140	0.5098
Pure Error	0.0012	4			0.0008	4		
Cor Total	0.1392	12			0.4170	12		
R^2	0.9832				R^2	0.9968		
Adjusted R^2	0.9712				Adjusted R^2	0.9946		
AP	24.891				AP	53.817		

SS = Sum of Square; AP = Adequate precision; df = degree of freedom.

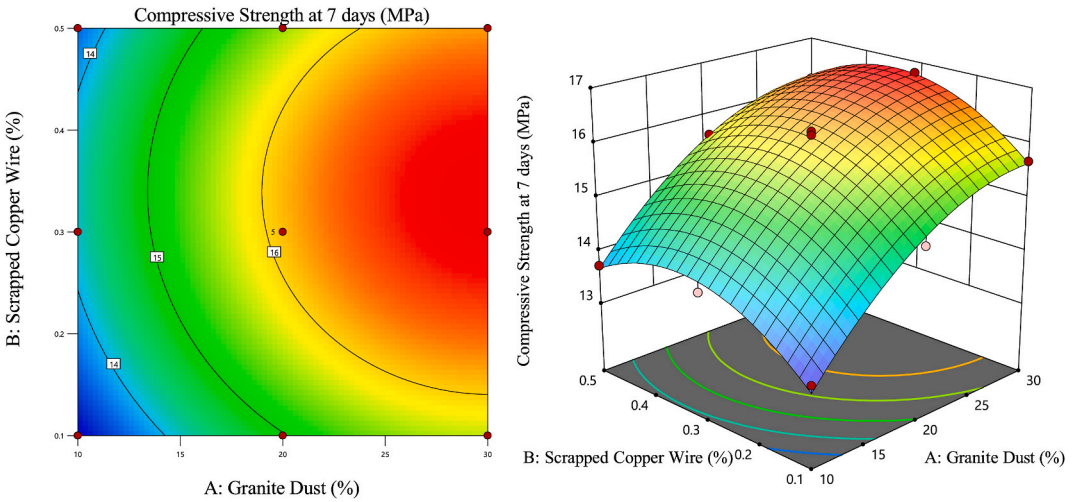

Fig. 4. Contours and 3D surface plot of RSM for compressive strength at 7 days.

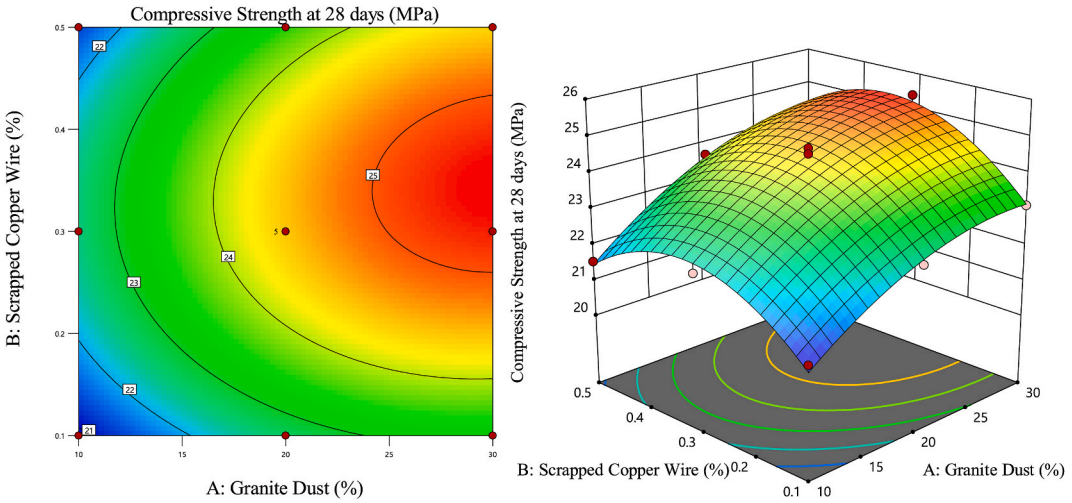

Fig. 5. Contours and 3D surface plot of RSM for compressive strength at 28 days.

the f_{st} rise with GD mixes up to 20 % and then starts to fall as more GD contents are added. Similar behavior of concrete consisting of GD was perceived by Aliabdo et al. [55] and Ghannam et al. [13]. The strength reduction phenomenon can be related to the requirement for more cement volume, which results from the cement and aggregate's poor interlocking [58]. The attributes of interfacial transition zones (ITZs) have impacts on the tensile strength of concrete, which in the case of GD does not need a significant amount of energy for crack expansions under tensile loading [56]. Therefore, the bond strength between aggregates and cement was reduced due to the use of GD [57]. The addition of SCW shows a higher splitting tensile strength of up to 0.5 % of substitution in the concrete mix. However, the rate of increment begins to decrease beyond a certain limit (0.3 %). The inclusion of distorted fibers may lead to an interlocking network of particles due to mechanical anchoring. Accordingly, fiber with a stronger link to the concrete mixture performs better in terms of tensile strength [59]).

3.3. Statistical analysis of the models

Table 9 presents the various statistical parameters utilized for assessing the effectiveness of predictive models. The model accuracy is determined with regard to coefficient of correlation (R), mean absolute error (MAE), mean square error (MSE), coefficient of determination (R^2), root mean square error (RMSE), absolute error (AE), standard error prediction (SEP) for all responses. The coefficient of determination (R^2) is a universal indication of a model's competence [60,61] and is used to examine the model's integrity. Table 9 indicates that the R^2 value for all responses ranges from 0.9832 to 0.9968 > 0.9 and is close to 1.0, demonstrating a great degree of relation between the observed and predicted data [62]. The MSE values for four responses (0.01576, 0.02385, 0.00018, and

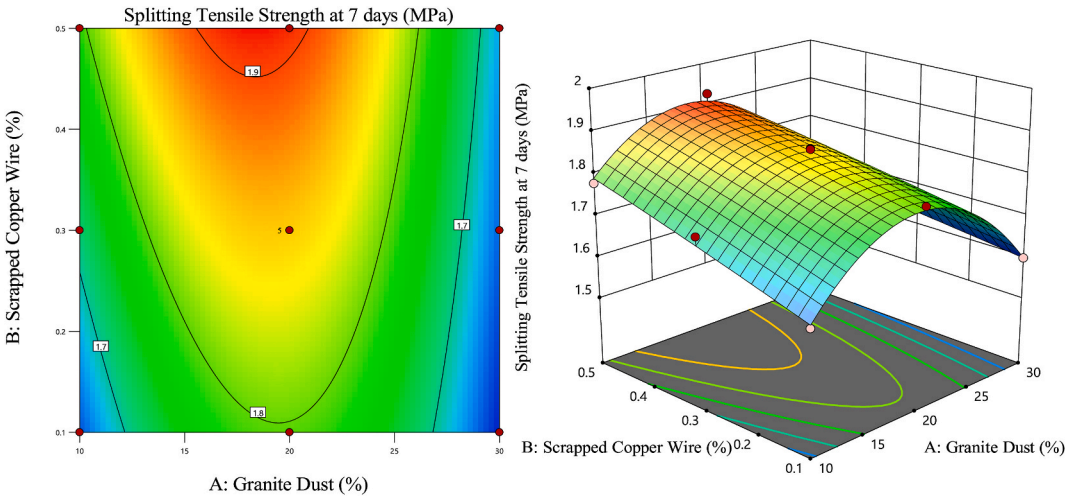

Fig. 6. Contours and 3D surface plot of RSM for splitting tensile strength at 7 days.

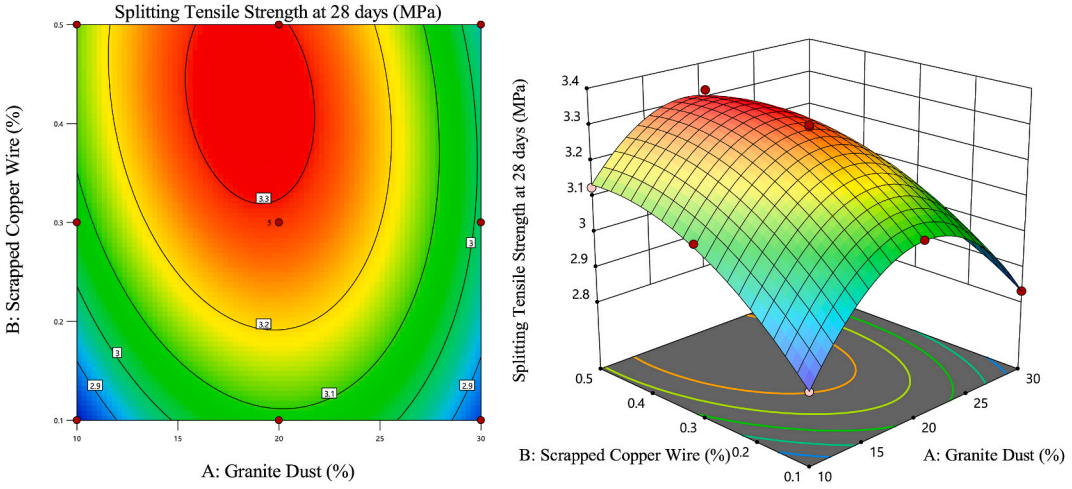

Fig. 7. Contours and 3D surface plot of RSM for splitting tensile strength at 28 days.

Table 9
Statistical parameters of the RSM model.

	R	R^2	MSE	RMSE	MAE	AE	SEP
$f'_{c,7}$	0.9939	0.9879	0.01576	0.12553	0.0939	0.0260769	0.8148
$f'_{c,28}$	0.9929	0.9858	0.02385	0.15443	0.1288	−0.0153846	0.6546
$f_{st,7}$	0.9916	0.9832	0.00018	0.01341	0.0099	0.00000076	0.7572
$f_{st,28}$	0.9984	0.9968	0.00010	0.01009	0.0082	−0.0000015	0.3234

0.00010) indicate non-significant residual errors (Table 9). When anticipated findings are compared to observed values, the AE values for f'_c and f_{st} are 0.0260769 and 0.00000076, respectively, which implies these two models were slightly overpredicted. In contrast, the values of MSE were 0.0153846 less for f'_c and 0.0000015 less for f_{st} at 28 days. The parameter MAE interprets that the anticipated values for f'_c and f_{st} differed by 0,0939, 0.1288, 0.0099, and 0.0082 from empirically obtained results at 7 and 28 days, respectively. These outcomes show that the models can accurately simulate the hardened strength of concrete [63].

3.4. Optimization and validation

In this study, the optimization approach analyzed all four responses concurrently to reach a suitable concrete mix design for all studied responses. When analyzing several responses, it is critical to figure out the adjustable optimum, which does not enhance only a

Table 10
Optimization benchmark of responses and variables considering the standard error models.

Name	Goal	Lower Limit	Upper Limit	Lower Weight	Upper Weight	Importance
A: GD	maximize	10	30	1	1	5
B: SCW	is in range	0.1	0.5	1	1	5
$f'_{c,7}$	maximize	13.15	16.79	1	1	5
StdErr ($f'_{c,7}$)	minimize	0.054782	0.117281	1	1	5
$f'_{c,28}$	maximize	21.06	25.37	1	1	5
StdErr ($f'_{c,28}$)	minimize	0.076607	0.164005	1	1	5
$f_{st,7}$	maximize	1.598	1.924	1	1	5
StdErr ($f_{st,7}$)	minimize	0.007586	0.01624	1	1	5
$f_{st,28}$	maximize	2.801	3.321	1	1	5
StdErr ($f_{st,28}$)	minimize	0.005713	0.012231	1	1	5

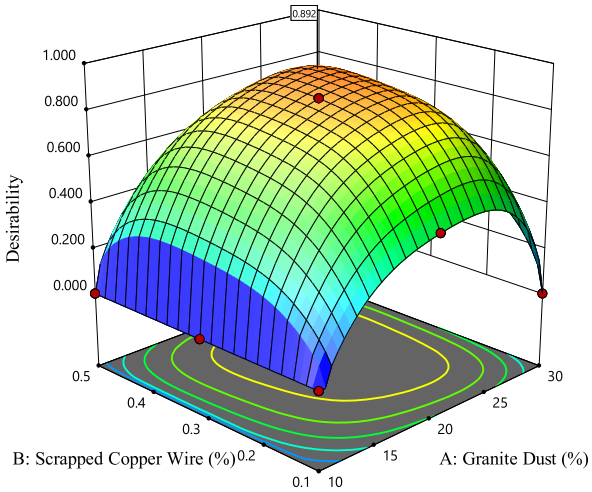

Fig. 8. Desirability zone concerning GD and SCW.

single response [64]. Here two different approaches are taken to optimize the responses. One includes standard error models and the other one without standard error models. The goal is to achieve the utmost f'_c , f_{st} , and standard error model minimization with maximum GD and in-range SCW usage (see Table 10). The optimization method yielded several possible solutions. However, the combination of 23.32 % GD replacement and 0.37 % SCW inclusion produced the maximum desirability of 0.892. (Fig. 8). Desirability is a mathematical strategy for determining the best solution, where the value 0 indicates that the factors offer an unfavorable reaction and the value 1 is assigned when the factors function optimally [65,66].

Experiments were performed with the optimal proportion of GD and SCW contents (23.32 % GD and 0.37 % SCW) to validate the predicted optimal result generated by RSM. Table 11 demonstrates the empirical and optimized f'_c and f_{st} values at 7 and 28 days. Values derived from 7 day and 28 day f'_c tests were closely matched to the predicted values upon validation, whereas a slight variation in predicted values was observed from experimental values for f_{st} at 7 and 28 days.

4. Conclusion

The prior objective of this research work is to investigate the influences of incorporating two recycled waste materials- GD as a potential fine aggregate replacement and SCW as a fiber reinforcement in concrete to diminish the demand for natural resources as well as to develop a sustainable way. RSM has been implemented to build mathematical models to predict concrete strength and achieve an optimal mix percentage of GD and SCW. The results of the ANOVA were used to analyze the impact of each variable on the responses. The following consequential statements can be concluded from the earlier discussion:

4.1. Important findings

- The 30 % replacement of natural sand with GD and 0.3 % inclusion of SCW fiber yields the maximal $f'_{c,7}$ having 16.90 MPa and $f'_{c,28}$ having 25.37 MPa. However, there is a decreasing pattern beyond that SCW percentage.
- The 20 % replacement of natural sand with GD and 0.5 % inclusion of SCW fiber in concrete yields the maximum $f_{st,7}$ having 1.924 MPa and $f_{st,28}$ having 3.321 MPa. If the inclusion of GD increases by more than 20 %, the splitting tensile strength decreases.

Table 11
Predicted strength by RSM and validation upon response surface values.

	Predicted Values	Experimental Result
A: GD (%)	23.32	
B: SCW (%)	0.37	
$f'_{c,7}$ (MPa)	16.48	16.01
$f'_{c,28}$ (MPa)	24.89	25.51
$f_{st,7}$ (MPa)	1.838	1.685
$f_{st,28}$ (MPa)	3.266	2.927
Desirability	0.892	

- All the models established by RSM were significant, as acceptable statistical values were found. The RSM-created regression model shows considerable preciseness and is capable of predicting the mechanical attributes of the concrete mixture.
- The multi-objective optimization produced optimal levels of the variables (23.32 % GD and 0.37 % SCW) that could accomplish desired properties without affecting any of the responses. The observed and predicted values of the responses are closely matched during the empirical validation of the developed models. This indicates that RSM can predict and analyze the effects of test variables on responses.

4.2. Limitations and recommendations for future studies

To assess the performance of GD and SCW mixed concrete in structural members, a comprehensive flexural strength test, shear strength test, and exploration of deflection properties in concrete beams and slabs should be conducted. In addition, the functionality of GD and SCW utilized prestressed concrete members subjected to static and fatigue loading should also be studied. In future investigations, a comprehensive study can be performed to explore the mechanical and physical properties, and durability of GD and SCW obtained concrete. Aspects such as bond strength, toughness, internal shrinkage, drying shrinkage, creep, leaching behavior, frost, electrical, and fire resistance, and water absorption properties of GD and SCW concrete should be considered. Exploring data on compressive strength at 14 days and 56 days will enhance the understanding of concrete's strength development. The investigation can be broadened by examining a wider range of GD and SCW percentages. Moreover, crack analysis for GD and SCW mixed concrete needs to be rigorously explored for practical implementation.

4.3. Contribution to practice, science, and policy

Even though standard ACI codes are globally followed for the exercise of ordinary concrete, no standardization has been established for alternatives replacing conventional materials or the addition of different fiber reinforcements. This study can serve as a guideline for reinforcing SCW in concrete matrix along with replacing typical fine aggregate with GD in construction applications. In developing nations, where managing a large amount of solid waste is a challenge, encouraging the utilization of such improperly disposed GD and recycling SCW in concrete can be a solution. Owing to the fact that it not only enhances concrete properties but also paves the way to a greener and more sustainable environment.

CRediT authorship contribution statement

Mohaiminul Haque: Supervision, Software, Resources, Project administration, Funding acquisition, Data curation. **Sourav Ray:** Writing – review & editing, Visualization, Validation, Supervision, Software, Resources, Project administration, Methodology, Funding acquisition, Data curation, Conceptualization. **Ayesha Ferdous Mita:** Writing – review & editing, Supervision, Software, Resources, Investigation, Formal analysis. **Anik Mozumder:** Writing – original draft, Investigation, Data curation. **Tirtha Karmaker:** Writing – original draft, Investigation, Data curation. **Sanjida Akter:** Investigation, Data curation.

Declaration of competing interest

The authors declare that they have no known competing financial interests or personal relationships that could have appeared to influence the work reported in this paper.

Acknowledgements

This research was funded by the SUST research center, Shahjalal University of Science and Technology, Sylhet, Bangladesh [Project code: AS/2020/1/13].

References

[1] K. Al-Zboon, J. Al-Zou'by, Recycling of stone cutting slurry in concrete mixes, J. Mater. Cycles Waste Manag. 17 (2015) 324–335, https://doi.org/10.1007/s10163-014-0246-x.

[2] F.M. Khalaf, A.S. DeVenny, Recycling of Demolished masonry rubble as coarse aggregate in concrete: review, J. Mater. Civ. Eng. 16 (2004) 331–340, https://doi.org/10.1061/(ASCE)0899-1561(2004)16:4(331).

[3] M. Moini, I. Flores-Vivian, A. Amirjanov, K. Sobolev, The optimization of aggregate blends for sustainable low cement concrete, Construct. Build. Mater. 93 (2015) 627–634, https://doi.org/10.1016/j.conbuildmat.2015.06.019.

[4] M. Chitlange, P. Pajgade, Strength appraisal of artificial sand as fine aggregate in SFRC, ARPN J. Eng. Appl. Sci. 5 (2010) 34–38.

[5] S.B. Kim, N.H. Yi, H.Y. Kim, J.-H.J. Kim, Y.-C. Song, Material and structural performance evaluation of recycled PET fiber reinforced concrete, Cem. Concr. Compos. 32 (2010) 232–240.

[6] L.W. Zhang, A.O. Sojobi, V.K.R. Kodur, K.M. Liew, Effective utilization and recycling of mixed recycled aggregates for a greener environment, J. Clean. Prod. 236 (2019) 117600, https://doi.org/10.1016/j.jclepro.2019.07.075.

[7] A.O. Sojobi, O.J. Aladegboye, T.F. Awolusi, Green interlocking paving units, Construct. Build. Mater. 173 (2018) 600–614, https://doi.org/10.1016/j.conbuildmat.2018.04.061.

[8] A.O. Sojobi, T.F. Awolusi, G.B. Aina, O.L. Oke, M. Oladokun, D.O. Oguntayo, Ternary and quaternary blends as partial replacement of cement to produce hollow sandcrete blocks, Heliyon 7 (2021).

[9] A.O. Sojobi, Evaluation of the performance of eco-friendly lightweight interlocking concrete paving units incorporating sawdust wastes and laterite, Cogent Eng 3 (2016) 1255168, https://doi.org/10.1080/23311916.2016.1255168.

[10] W.E. Elemam, I.S. Agwa, A.M. Tahwia, Reusing ceramic waste as a fine aggregate and supplemental cementitious material in the manufacture of sustainable concrete, Buildings 13 (2023), https://doi.org/10.3390/buildings13112726.

[11] A.H.A. Walid E. Elemam Mohamed G. Mahdy and Ahmed M. Tahwia, Prediction and Optimization of Self-Consolidating Concrete Properties, ACI Mater J. 119 (n.d.). https://doi.org/10.14359/51733149..

[12] A.E.M. Abd Elmoaty, Mechanical properties and corrosion resistance of concrete modified with granite dust, Construct. Build. Mater. 47 (2013) 743–752, https://doi.org/10.1016/J.CONBUILDMAT.2013.05.054.

[13] N. Zainuddin, N.Z. Mohd Yunus, M.A.M. Al-Bared, A. Marto, I.S.H. Harahap, A.S.A. Rashid, Measuring the engineering properties of marine clay treated with disposed granite waste, Measurement 131 (2019) 50–60, https://doi.org/10.1016/j.measurement.2018.08.053.

[14] L. Gautam, J.K. Jain, P. Kalla, M. Danish, Sustainable utilization of granite waste in the production of green construction products: a review, Mater. Today Proc. 44 (2021) 4196–4203, https://doi.org/10.1016/j.matpr.2020.10.53.

[15] S. Ghorbani, I. Taji, J. de Brito, M. Negahban, S. Ghorbani, M. Tavakkolizadeh, A. Davoodi, Mechanical and durability behaviour of concrete with granite waste dust as partial cement replacement under adverse exposure conditions, Construct. Build. Mater. 194 (2019) 143–152, https://doi.org/10.1016/j.conbuildmat.2018.11.023.

[16] G. Garas, Studies undertaken to incorporate marble and granite wastes in green concrete production, ARPN 9 (2014) 1559–1564.

[17] S. Ghannam, H. Najm, R. Vasconez, Experimental study of concrete made with granite and iron powders as partial replacement of sand, Sustainable Materials and Technologies 9 (2016) 1–9, https://doi.org/10.1016/j.susmat.2016.06.001.

[18] L.K. Gupta, A.K. Vyas, Impact on mechanical properties of cement sand mortar containing waste granite powder, Construct. Build. Mater. 191 (2018) 155–164, https://doi.org/10.1016/j.conbuildmat.2018.09.203.

[19] S. Singh, R. Nagar, V. Agrawal, A review on Properties of Sustainable Concrete using granite dust as replacement for river sand, J. Clean. Prod. 126 (2016) 74–87, https://doi.org/10.1016/j.jclepro.2016.03.114.

[20] S. Upadhyaya, B. Nanda, R. Panigrahi, Experimental analysis on partial replacement of fine aggregate by granite dust in concrete, in: Lecture Notes in Civil Engineering, Springer, 2019, pp. 335–344, https://doi.org/10.1007/978-981-13-3317-0_31.

[21] P. Nuaklong, P. Worawatnalunart, P. Jongvivatsakul, S. Tangaramvong, T. Pothisiri, S. Likitlersuang, Pre- and post-fire mechanical performances of high calcium fly ash geopolymer concrete containing granite waste, J. Build. Eng. 44 (2021) 103265, https://doi.org/10.1016/J.JOBE.2021.103265.

[22] A. Jain, S. Chaudhary, R. Gupta, Mechanical and microstructural characterization of fly ash blended self-compacting concrete containing granite waste, Construct. Build. Mater. 314 (2022) 125480.

[23] Y. Divakar, M. Amalkar, A. Uddappa, Experimental investigation on behaviour of concrete with the use of granite fines, International Journal of Advanced Engineering Research and Studies 1 (2012) 84–87.

[24] A. Anbu, Strength and durability properties of granite powder concrete, J. Civ. Eng. Res. 4 (2014) 1–6.

[25] S. Singh, S. Khan, R. Khandelwal, A. Chugh, R. Nagar, Performance of sustainable concrete containing granite cutting waste, J. Clean. Prod. 119 (2016) 86–98, https://doi.org/10.1016/j.jclepro.2016.02.008.

[26] K.C. Williams, P. Partheeban, F.T. Kala, Mechanical properties of high performance concrete incorporating granite powder as fine aggregate, Int. J. Des. Manuf. Technol. 2 (2008) 67–73.

[27] F.K. Thomas, P. Partheeban, Study on the Effect of Granite Powder on Concrete Properties, 2015, pp. 63–70, https://doi.org/10.1680/COMA.2010.163.2.63.

[28] C. Suresh, S. Sivaramakrishnan, P. Siddharthan, S. Vinay Babu, V. Sai Neeraja, J. Arockia Dhanraj, Study on the characteristics of the ordinary concrete with the granite dust as a substitute for the fine aggregates, Mater. Today Proc. (2022), https://doi.org/10.1016/j.matpr.2022.07.154.

[29] M. di Prisco, G. Plizzari, L. Vandewalle, Fibre reinforced concrete: new design perspectives, Mater. Struct. 42 (2009) 1261–1281, https://doi.org/10.1617/s11527-009-9529-4.

[30] B. Schnůtgen, L. Vandewalle, Test and design methods for steel fibre reinforced concrete–background and experiences, in: Proceeding of the RILEM TC 162-TDF Workshop, 2003.

[31] R.P. Borg, O. Baldacchino, L. Ferrara, Early age performance and mechanical characteristics of recycled PET fibre reinforced concrete, Construct. Build. Mater. 108 (2016) 29–47, https://doi.org/10.1016/j.conbuildmat.2016.01.029.

[32] D.J. Kim, S.H. Park, G.S. Ryu, K.T. Koh, Comparative flexural behavior of hybrid ultra high performance fiber reinforced concrete with different macro fibers, Construct. Build. Mater. 25 (2011) 4144–4155.

[33] F. Bencardino, L. Rizzuti, G. Spadea, R.N. Swamy, Experimental evaluation of fiber reinforced concrete fracture properties, Compos. B Eng. 41 (2010) 17–24.

[34] S.H. Park, D.J. Kim, G.S. Ryu, K.T. Koh, Tensile behavior of ultra high performance hybrid fiber reinforced concrete, Cem. Concr. Compos. 34 (2012) 172–184.

[35] T.F. Awolusi, O.L. Oke, O.O. Akinkurolere, A.O. Sojobi, Application of response surface methodology: predicting and optimizing the properties of concrete containing steel fibre extracted from waste tires with limestone powder as filler, Case Stud. Constr. Mater. 10 (2019), https://doi.org/10.1016/j.cscm.2018.e00212.

[36] A.M. Tahwia, M. Mokhles, W.E. Elemam, Optimizing characteristics of high-performance concrete incorporating hybrid polypropylene fibers, Innovative Infrastructure Solutions 8 (2023) 297, https://doi.org/10.1007/s41062-023-01268-6.

[37] Y. Wang, H.C. Wu, V.C. Li, Concrete reinforcement with recycled fibers, J. Mater. Civ. Eng. 12 (2000) 314–319.

[38] T.R. Martins, N.S. Mrozinski, D.A. Bertuol, E.H. Tanabe, Recovery of copper and aluminium from coaxial cable wastes using comparative mechanical processes analysis, Environ. Technol. 0 (2020) 1–13, https://doi.org/10.1080/09593330.2020.1725141.

[39] M. Koushkbaghi, M.J. Kazemi, H. Mosavi, E. Mohseni, Acid resistance and durability properties of steel fiber-reinforced concrete incorporating rice husk ash and recycled aggregate, Construct. Build. Mater. 202 (2019) 266–275, https://doi.org/10.1016/j.conbuildmat.2018.12.224.

[40] A. Arjomandi, R. Mousavi, M. Tayebi, M. Nematzadeh, A. Gholampour, A. Aminian, O. Gencel, The effect of sulfuric acid attack on mechanical properties of steel fiber-reinforced concrete containing waste nylon aggregates: experiments and RSM-based optimization, J. Build. Eng. 64 (2023) 105500, https://doi.org/10.1016/j.jobe.2022.105500.

[41] O. Zaid, F. Alsharari, F. Althoey, A.B. Elhag, H.M. Hadidi, M.A. Abuhussain, Assessing the performance of palm oil fuel ash and Lytag on the development of ultra-high-performance self-compacting lightweight concrete with waste tire steel fibers, J. Build. Eng. 76 (2023) 107112, https://doi.org/10.1016/j.jobe.2023.107112.

[42] L. Bertolini, B. Elsener, P. Pedeferri, E. Redaelli, R.B. Polder, Corrosion of Steel in Concrete: Prevention, Diagnosis, Repair, John Wiley & Sons, 2013.

[43] J.-L. Granju, S. Balouch, Corrosion of steel fibre reinforced concrete from the cracks, Cement Concr. Res. 35 (2005) 572–577, https://doi.org/10.1016/j.cemconres.2004.06.032.
[44] A.M. Shende, A.M. Pande, M.G. Pathan, Experimental Study on Steel Fiber Reinforced Concrete for M-40 Grade, 2012. www.irjes.comwww.irjes.com.
[45] Ş. Yazıcı, G. İnan, V. Tabak, Effect of aspect ratio and volume fraction of steel fiber on the mechanical properties of SFRC, Construct. Build. Mater. 21 (2007) 1250–1253.
[46] MdH.R. Sobuz, A. Saha, J.F. Anamika, M. Houda, M. Azab, A.S.M. Akid, MdJ. Rana, Development of self-compacting concrete incorporating rice husk ash with waste galvanized copper wire fiber, Buildings 12 (2022), https://doi.org/10.3390/buildings12071024.
[47] L.V. Candioti, M.M. de Zan, M.S. Cámara, H.C. Goicoechea, Experimental design and multiple response optimization. Using the desirability function in analytical methods development, Talanta 124 (2014) 123–138.
[48] M.A. Bezerra, R.E. Santelli, E.P. Oliveira, L.S. Villar, L.A. Escaleira, Response surface methodology (RSM) as a tool for optimization in analytical chemistry, Talanta 76 (2008) 965–977, https://doi.org/10.1016/J.TALANTA.2008.05.019.
[49] A.I. Khuri, S. Mukhopadhyay, Response Surface Methodology, vol. 2, Wiley Interdiscip Rev Comput Stat., 2010, pp. 128–149, https://doi.org/10.1002/WICS.73.
[50] B.S. Kaith, R. Sharma, S. Kalia, M.S. Bhatti, Response surface methodology and optimized synthesis of guar gum-based hydrogels with enhanced swelling capacity, RSC Adv. 4 (2014) 40339–40344, https://doi.org/10.1039/C4RA05300A.
[51] W.E. Elemam, A.M. Tahwia, M. Abdellatief, O. Youssf, M.A. Kandil, Durability, microstructure, and optimization of high-strength geopolymer concrete incorporating construction and demolition waste, Sustainability 15 (2023), https://doi.org/10.3390/su152215832.
[52] M. Haque, S. Ray, A.F. Mita, S. Bhattacharjee, MdJ. bin Shams, Prediction and optimization of the fresh and hardened properties of concrete containing rice husk ash and glass fiber using response surface methodology, Case Stud. Constr. Mater. 14 (2021) e00505, https://doi.org/10.1016/j.cscm.2021.e00505.
[53] B. Şimşek, Y.T. İç, E.H. Şimşek, A RSM-based multi-response optimization application for determining optimal mix proportions of standard ready-mixed concrete, Arabian J. Sci. Eng. 41 (2016) 1435–1450.
[54] H. Amiri, S. Azadi, M. Karimaei, H. Sadeghi, Farshad Dabbaghi, Multi-objective optimization of coal waste recycling in concrete using response surface methodology, J. Build. Eng. 45 (2022) 103472, https://doi.org/10.1016/j.jobe.2021.103472.
[55] A. Botchkarev, A new typology design of performance metrics to measure errors in machine learning regression algorithms, Interdiscipl. J. Inf. Knowl. Manag. 14 (2019) 45–76, https://doi.org/10.28945/4184.
[56] S. Nakagawa, P.C.D. Johnson, H. Schielzeth, The coefficient of determination R2 and intra-class correlation coefficient from generalized linear mixed-effects models revisited and expanded, J R Soc Interface 14 (2017) 20170213, https://doi.org/10.1098/rsif.2017.0213.
[57] C.J. Willmott, K. Matsuura, Advantages of the mean absolute error (MAE) over the root mean square error (RMSE) in assessing average model performance, Clim. Res. 30 (2005) 79–82, https://doi.org/10.3354/CR030079.
[58] T. Ahmed, S. Ray, M. Haque, T. Tasnim Nahin, A. Ferdous Mita, Optimization of properties of concrete prepared with waste glass aggregate and condensed milk can fiber using response surface methodology, Clean Eng Technol 8 (2022) 100478, https://doi.org/10.1016/J.CLET.2022.100478.
[59] M.G. Larson, Analysis of variance, Circulation 117 (2008) 115–121, https://doi.org/10.1161/CIRCULATIONAHA.107.654335.
[60] A. Asfaram, M. Ghaedi, S. Agarwal, I. Tyagi, V. Kumar Gupta, Removal of basic dye Auramine-O by ZnS:Cu nanoparticles loaded on activated carbon: optimization of parameters using response surface methodology with central composite design, RSC Adv. 5 (2015) 18438–18450, https://doi.org/10.1039/C4RA15637D.
[61] M. Vijayalakshmi, A.S.S. Sekar, G. Ganesh prabhu, Strength and durability properties of concrete made with granite industry waste, Construct. Build. Mater. 46 (2013) 1–7, https://doi.org/10.1016/j.conbuildmat.2013.04.018.
[62] S. Singh, R. Nagar, V. Agrawal, A. Rana, A. Tiwari, Sustainable utilization of granite cutting waste in high strength concrete, J. Clean. Prod. 116 (2016) 223–235, https://doi.org/10.1016/j.jclepro.2015.12.110.
[63] T.K. Kim, Understanding one-way ANOVA using conceptual figures, Kja 70 (2017) 22–26, https://doi.org/10.4097/kjae.2017.70.1.22.
[64] P.S. Song, S. Hwang, Mechanical properties of high-strength steel fiber-reinforced concrete, Construct. Build. Mater. 18 (2004) 669–673, https://doi.org/10.1016/j.conbuildmat.2004.04.027.
[65] S. Ray, M. Haque, T. Ahmed, A.F. Mita, M.H. Saikat, M.M. Alom, Predicting the strength of concrete made with stone dust and nylon fiber using artificial neural network, Heliyon 8 (2022) e09129, https://doi.org/10.1016/j.heliyon.2022.e09129.
[66] A.A. Aliabdo, A.E.M. Abd Elmoaty, E.M. Auda, Re-use of waste marble dust in the production of cement and concrete, Construct. Build. Mater. 50 (2014) 28–41, https://doi.org/10.1016/j.conbuildmat.2013.09.005.